

1 A Hybrid Model Based on Grey Wolf Optimizer 2 and Lagrangian Support Vector Regression for 3 European Natural Gas Consumption 4 Forecasting

15 Abstract

With the intensification of the Russia-Ukraine war, there is a large-scale energy shortage in Europe, and the natural gas supply in Europe has a natural gas crisis due to the cut-off of the Nord Stream No.1 pipeline. Therefore, it is necessary to accurately predict the consumption of natural gas. In order to fulfill this requirement, this paper uses the Lagrangian Support Vector Regression model with *Sorensen* kernel based on the Nonlinear Auto-Regressive model and Grey Wolf Optimizer for 5-step forecasting of monthly natural gas consumption in all European countries. Under three time lags, comparing the 5-step predict results of *GWO-LSVR* with *SVR*, *RF*, *LightGBM*, *XGBoost*, and *MLP*, those five models' hyperparameters also optimized by *GWO*, it found that *GWO-LSVR* has smallest *MAPE* in almost all cases, and the numerical results of *MAPE* generated by *GWO-LSVR* is from 5.844% to 11.622%, the smaller the forecasting step size, the better the effect. Moreover, compares the difference of *GWO* and *WOA*, it is found that *GWO* can obtained better model hyperparameters and smaller *MAPE* results. To sum up, the proposed *GWO-LSVR* model has strong generalization performance and robustness, and is a reliable natural gas consumption prediction model.

16

17 *Keywords: Lagrangian Support Vector Regression; Grey Wolf Optimizer; Nonlinear Auto-*
18 *Regressive; Kernel Learning; Natural Gas Consumption in Europe.*

19 1. Introduction

20 As a clean and efficient low-carbon energy, natural gas is a very important part of the global
21 energy structure, accounting for about 25% of European energy consumption. Coupled with
22 the intensification of the situation in Russia and Ukraine, there is a serious shortage of
23 natural gas supply in Europe. Therefore, it is necessary to accurately predict the
24 consumption of natural gas [1].

25 Forecasting is the basis for understanding and decision-making, and natural gas
26 consumption forecasting is based on dynamic analysis of dynamic natural gas data models
27 and quantitative calculations on a qualitative basis. The analysis of natural gas consumption
28 data is a multidimensional time series analysis, which often implies a large number of
29 dynamic characteristics, and the mechanism of each factor cannot be described
30 quantitatively, so the forecasting of natural gas consumption is a complex non-linear problem,

31 and the accuracy of multidimensional time series forecasting is still a great challenge, and
 32 the development of high-precision multidimensional time series forecasting analysis methods
 33 is of great significance [2]. Box and Jenkins and Hannan were the first to propose the
 34 classical linear multidimensional time series analysis model, the controlled autoregressive
 35 integrating moving average (*CARMA*) [3][4], Boker and Keviczky gave their fixed-order F-test
 36 discriminant method [5]. Deng Zili and Guo Yixin further developed the F-test discriminant for
 37 order, suborder and time lag, forming a complete identification of the structure of the *CARMA*
 38 model and giving its simplified form, the controlled autoregressive (*CAR*) model with
 39 controlled terms [6]. and artificial neural networks (*ANN*) with good nonlinear approximation
 40 capability [7]. However, the selection of metrics in these traditional forecasting methods is
 41 arbitrary and the requirements for parameter selection and correction are high. Vapnik's
 42 support vector machine (*SVM*) [8], which is based on statistical learning theory, is the fastest
 43 growing machine learning method and was originally used for pattern recognition (*SVC*), with
 44 the introduction of the ε -insensitive loss function, it has been extended to be used for
 45 nonlinear time series analysis or nonlinear regression analysis (*SVR*) [9][10][11]; *SVR* is
 46 based on structural risk minimisation, which better solves the problems of small samples,
 47 nonlinearity, overfitting, dimensional disaster and office minimum, etc., with excellent
 48 generalisation and propagation ability In addition, it well solves the problems faced by the
 49 above methods, and has good performance in practical applications. However, *SVR* still has
 50 some limitations in practical applications. First, the selection of its kernel functions is
 51 empirical. Second, the selection of the corresponding parameters of some *SVR* programs is
 52 empirical and their kernel functions is also empirical [12]. Third, like *ANNs*, *SVR* models are less
 53 interpretable [13]. The limitations of *SVR* are overcome, or partially overcome, by dynamic
 54 selection of kernel functions [14][15] and forced screening of variables and giving the relative
 55 order of importance of variables in the order of elimination to give partial interpretability to
 56 the *SVR*. Thus, a non-linear multi-dimensional time series forecasting method based on
 57 *LSVR*, incorporating time series analysis and regression analysis, is developed for
 58 forecasting natural gas consumption in European countries, and the accuracy of the forecast
 59 can be guaranteed.

60 2. Design of the Forecasting Model

61 In this section, the detailed mathematical model of the *LSVR* (Lagrangian Support Vector
 62 Regression) with *Sorensen* kernel and the GWO (Grey Wolf Optimizer) used in this paper
 63 will be presented in **Section 2.1** and **Section 2.2**, respectively. And the complete multi-step
 64 forecasting model based on *NAR* (Nonlinear Auto-Regressive) model as out-of-sample
 65 holdout validation will be shown in **Section 2.3**.

67 2.1 Lagrangian Support Vector Regression with *Sorensen* kernel

68 The standard *SVR* formulation is a constrained, quadratic optimization problem, written in
 69 matrix form is as follows:
 70

$$71 \min \frac{1}{2} w^t w + v(e^t \xi + e^t \xi^*)$$

$$72 \text{ s. t. } \begin{cases} y - Aw - be \leq \varepsilon e + \xi \\ Aw + be - y \leq \varepsilon e + \xi^* \end{cases} \quad (1)$$

73 where $\xi_i, \xi_i^* \geq 0$ for $i = 1, 2, \dots, m$, ξ and ξ^* are the slack variables, t represents the
 74 transpose of the matrix, matrix $A \in R^{m \times n}$, *LSVR* has made two changes on the basis of *SVR*:

- 75 (1) Change ξ and ξ^* in 1-norm to be the square of 2-norm, which makes make it
 76 unnecessary for the slack variable to be greater than 0.
- 77 (2) Add b^2 to $w^t w$ in **Eq(1)**.

79 Thus the *LSVR* can be formulated as the following form:
80

$$81 \quad \min \frac{1}{2}(w^t w + b^2) + \frac{v}{2} \sum_{i=1}^m (\xi_i^2 + \xi_i^{*2}) \quad (2)$$

$$s. t. \begin{cases} y_i - A_i w - b \leq \varepsilon + \xi_i \\ A_i w + b - y_i \leq \varepsilon + \xi_i^* \end{cases}$$

82 where ε and v are the input parameters.
83

84 To solve the convex quadratic problem above, introducing two Lagrange multiplies $u_1 =$
85 $(u_{11}, u_{12}, \dots, u_{1m})^t$ and $u_2 = (u_{21}, u_{22}, \dots, u_{2m})^t$, the Lagrangian Function L can be obtained
86 as follows:
87

$$88 \quad L = \frac{1}{2}(w^t w + b^2) + \frac{v}{2} \sum_{i=1}^m (\xi_i^2 + \xi_i^{*2})$$

$$+ \sum_{i=1}^m u_{1i}(y_i - A_i w - b - \varepsilon - \xi_i) \quad (3)$$

$$+ \sum_{i=1}^m u_{2i}(A_i w + b - y_i - \varepsilon - \xi_i^*)$$

89 The optimality condition is that the partial derivative of L with respect to the original variable
90 is 0, we can obtained the solution of **Eq(3)**:
91

$$92 \quad w = A^t(u_1 - u_2) \text{ and } b = e^t(u_1 - u_2) \quad (4)$$

93 and the dual problem can be written as the minimization problem:
94

$$95 \quad \min \frac{1}{2}[(u_1 - u_2)^t(A^t A + ee^t)(u_1 - u_2)] + \frac{1}{2v}(u_1^t u_1 + u_2^t u_2) - y^t(u_1 - u_2) + \varepsilon e^t(u_1 + u_2) \quad (5)$$

96 The linear *LSVR* is the method to output a approximate function $f(\cdot)$, based on the **Eq(4)**, the
97 linear regression estimation function is given as:
98

$$99 \quad f(x) = [x \quad 1] \begin{bmatrix} A^t \\ e^t \end{bmatrix} (u_1 - u_2) \quad (6)$$

100 Define an augmented matrix $D = [A \quad e]$, the **Eq(5)** can be equally expressed as:
101

$$102 \quad \min \frac{1}{2} [u_1^t \quad u_2^t] M \begin{bmatrix} u_1 \\ u_2 \end{bmatrix} - p^t \begin{bmatrix} u_1 \\ u_2 \end{bmatrix} \quad (7)$$

103 where
104

$$105 \quad M = \begin{bmatrix} \frac{1}{v} + DD^t & -DD^t \\ -DD^t & \frac{1}{v} + DD^t \end{bmatrix} \quad (8)$$

106 and
107

108
109

$$114 \quad p = \begin{bmatrix} p_1 \\ p_2 \end{bmatrix} = \begin{bmatrix} y - \varepsilon e \\ -y - \varepsilon e \end{bmatrix} \quad (9)$$

115

116 The linear *LSVR* in **Eq(7)** can be extend to nonlinear model with kernel matrix K . In this
117 paper, we used the Sorensen kernel which expressed as the following form:

118

$$119 \quad K(u, v) = \frac{2u \cdot v}{\|u\|_2^2 + \|v\|_2^2} \quad (10)$$

120

121 where $u \cdot v$ is a inner product of the two vectors.

122 Replacing DD^t by $K = K(D, D^t)$ in **Eq(7)**, for any $x \in R^n$, the kernel regression estimation
123 function $f(\cdot)$ is obtained to be of the following form:

124

$$125 \quad f(x) = K([x^t \quad 1], D^t)(u_1 - u_2) \quad (11)$$

126

127 **2.2 Grey Wolf Optimizer**

128

129 The *GWO* algorithm is inspired the unique hunting and hierarchy behavior of the grey wolves.
130 Grey wolves have a very strict social dominant hierarchy, in order to mathematically model
131 the hierarchy in *GWO*, the best solution is α , the second and the third best solutions are β
132 and δ , and the rest of the candidate solutions called ω . The hunting behavior is divided into
133 two stages: Encircling and hunting for prey. The specific mathematical modeling steps for
134 the two stages are described below.

135

136 **Encircling:** The Grey wolves encircle the prey first when they hunt. The encircle behavior
137 modeled as follows:

138

$$139 \quad \vec{D} = |\vec{C} \cdot \vec{X}_p(l) - \vec{X}(l)| \quad (12)$$

140

$$141 \quad \vec{X}(l+1) = \vec{X}_p(l) - \vec{A} \cdot \vec{D} \quad (13)$$

142

143 where l represents the current iteration, \vec{X}_p is the position of the prey, \vec{X} is the position of a
144 grey wolf, and \vec{A} and \vec{C} are coefficient vectors, which calculated as follows:

145

$$146 \quad \vec{A} = 2\vec{a} \cdot \vec{r}_1 - \vec{a} \quad (14)$$

147

$$148 \quad \vec{C} = 2 \cdot \vec{r}_2 \quad (15)$$

149

150 where \vec{r}_1, \vec{r}_2 are random vectors in $[0, 1]$, the components of \vec{a} are linearly decreased from 2
151 to 0 during the course of iterations.

152

153 **Hunting:** The hunt of the prey always guided by the α wolf, sometimes, the β and δ wolf
154 participate in the hunt. Assume that the α , β and δ have better knowledge of the prey in the
155 abstract space. Therefore, save the best three solutions obtained so far, and update other
156 search agents' position (including ω) according to the position of the best search agents.
157 This progress is modeled as follows:

158

$$159 \quad \vec{X}_{1,2,3} = \vec{X}_{\alpha,\beta,\delta} - \vec{A}_{1,2,3} \cdot \vec{D}_{\alpha,\beta,\delta} \quad (16)$$

160

$$161 \quad \vec{X}(l+1) = \frac{\vec{X}_1 + \vec{X}_2 + \vec{X}_3}{3} \quad (17)$$

162

163 where $\vec{X}_{1,2,3}$ represents \vec{X}_1, \vec{X}_2 and \vec{X}_3 , $\vec{X}_{\alpha,\beta,\delta}$ represents $\vec{X}_\alpha, \vec{X}_\beta$ and \vec{X}_δ .

164

165 **2.3 Complete multi-step forecasting strategy based on NAR model**

166

167 In this section, the *NAR* model which can transform the original time series to supervised168 learning dataset will be given in **Section 2.3.1**, the out-of-sample holdout validation scheme169 presented in **Section 2.3.2**, and the complete algorithm flow will be shown in **Section 2.3.3**.

170

171 **2.3.1 Nonlinear Auto-Regressive model for multi-step forecasting**

172

173 A machine learning model is a class of models with high-dimensional inputs, Preferably

174 without using raw time series data as input. The Nonlinear Auto-Regressive (*NAR*) model is

175 a type of model that reconstructs the original data set based on phase space reconstruction

176 and lag methods. Given a Univariate times series data $U = \{u_1, u_2, u_3, \dots, u_n\}$, phase space177 reconstruction of U yields a new dataset Φ in **Eq(18)** for supervised learning, the new178 dataset (matrix: Φ) can be expressed as follows:

179

180

$$\Phi = \begin{pmatrix} u_1 & u_2 & \dots & u_\tau & u_{\tau+1} \\ u_2 & u_3 & \dots & u_{\tau+1} & u_{\tau+2} \\ \vdots & \vdots & \ddots & \vdots & \vdots \\ u_{n-\tau} & u_{n-\tau+1} & \dots & u_{n-1} & u_n \end{pmatrix} \quad (18)$$

181

182 Where τ is the time lag.

183

184 **2.3.2 out-of-sample holdout validation**

185

186 In this paper, we use the out-of-sample holdout validation to validate the best

187 hyperparameters of the model. Different with conventional *k-fold* cross-validation in machine

188 learning models, the out-of-sample holdout validation requires only one validation on the

189 validation set, *k-fold* cross-validation will disrupt the order of the data set when performing

190 multiple cross-validation, but there is a certain irrationality in the validation of the time series

191 model. Because it is unreasonable to validate past data with future data.

192

193 Split the reconstructed data set according to the ratio of about 8:1:1 according to the

194 sequence, the split datasets are training, validation, and test sets, respectively. First, the

195 default hyperparameters of *LSVR* are used to train the model on the training set, then *GWO*

196 will optimize the model hyperparameters on the validation set, and the final multi-step

197 forecasting process will be performed on the test set.

198

199

$$MAPE = \min \frac{1}{n} \sum \left| \frac{u_j - \hat{u}_j}{u_j} \right| \times 100\% \quad (19)$$

200

201 Throughout the process, we use *MAPE* which presents in **Eq(19)** as an indicator to evaluate202 model performance. The smaller the *MAPE*, the better the model performance.

203

204 **2.3.3 Complete multi-step forecasting model**

205

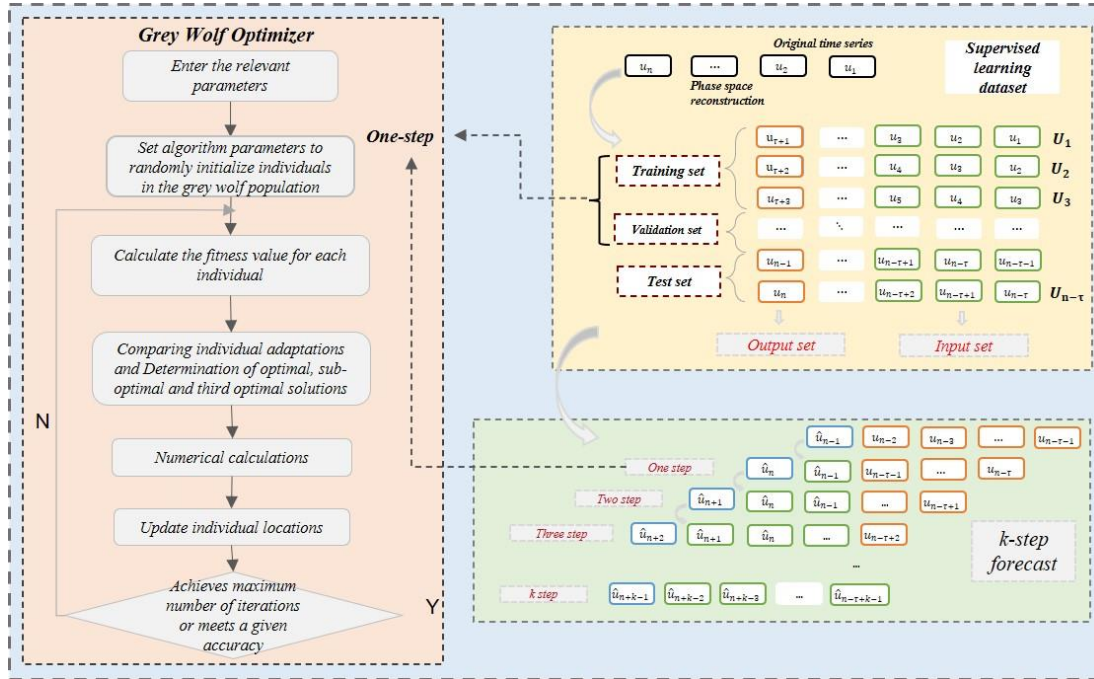
206 The completed multi-step forecasting model will be shown in this part. The detailed model

207 flow chart is shown in **Figure 1**, and the specific model prediction process is divided into the

208 following five steps:

209

- 210 (1) Phase space reconstruction of the original time series U into a supervised learning
- 211 dataset using NAR model.
- 212 (2) Split the dataset in a ratio of about 8:1:1.
- 213 (3) Train the $LSVR$ model on the training set with default hyperparameters.
- 214 (4) With the minimum $MAPE$ as the goal, use GWO for optimization on the validation set.
- 215 (5) Multi-step prediction on test set.
- 216



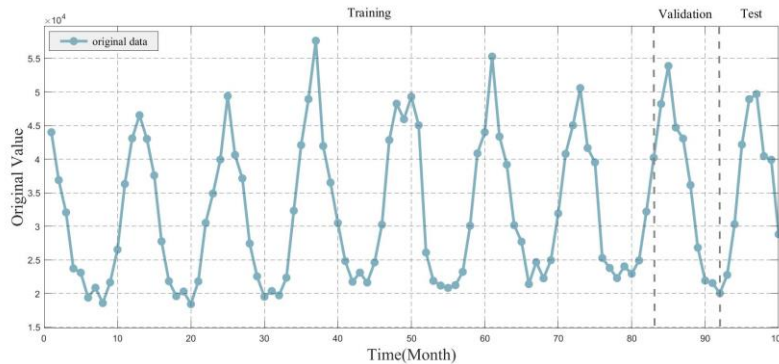
217
218

Figure 1 Complete algorithm flow

219 **3. Dataset Description**

220 In this paper, the dataset we used is from the publicly available European natural gas
 221 consumption (NGC) dataset in the Eurostat(<https://ec.europa.eu/eurostat>), which collects
 222 monthly NGC data from Jan 2014 to May 2022 for a total of 100 months. Total monthly
 223 natural gas consumption for a total of 27 countries within Europe. Use the first eighty points
 224 to train the $LSVR$ model, use the next ten points to find the optimal hyperparameters of the
 225 model, and use the last ten points for multi-step forecasting. The original dataset is shown in
 226 **Figure 2.**

227



228
229

Figure 2 Original dataset

230 4. Multi-Step Forecasting Results and Discussion

231 In this section, we compared *GWO-LSVR* with five machine learning models with high
 232 generalization performance at three different time lags. These five models include *SVR*
 233 similar to *LSVR*, tree models Random Forest (*RF*), Light Gradient Boosting Machine
 234 (*LightGBM*), and Extreme Gradient Boosting (*XGBoost*), neural network model Multilayer
 235 Perceptron (*MLP*). The modeling and optimization process of these five models is the same
 236 as *GWO-LSVR*. The detailed comparison results are shown in **Section 4.1**. The impact of
 237 different optimization algorithms on the results is discussed in **Section 4.2**.

238

239 4.1 Analysis of the multi-step forecasting results

240

241 In order to quantitatively analyze the performance of the model, the *MAPE* of multi-step
 242 forecasting is used as the evaluation standard. In all experiments, for a more comprehensive
 243 comparison of these models, three different lags (that is, $\tau=3$, $\tau=4$, $\tau=5$) were chosen. In the
 244 multi-step forecasting process, we predict 5 steps forward under the three time lags, and
 245 calculated the *MAPE* of each step.

246

247 Applying the proposed model to the forecast of monthly NGC for all countries on a European
 248 scale. The detailed *MAPE* results shown in **Table 1**. It can be plainly seen that from the table,
 249 the proposed *GWO-LSVR* model yields the minimal *MAPE* almost all cases. The numerical
 250 result of its *MAPE* is from 5.844% to 11.622%. Only when $\tau=4$, *GWO-XGBoost* has better
 251 *MAPE* than *GWO-LSVR* at the fourth step. But in this case, the results of the proposed model
 252 are better than the other four models. Detailed *MAPE* results also shown in **Figure 3**.

253

254

255

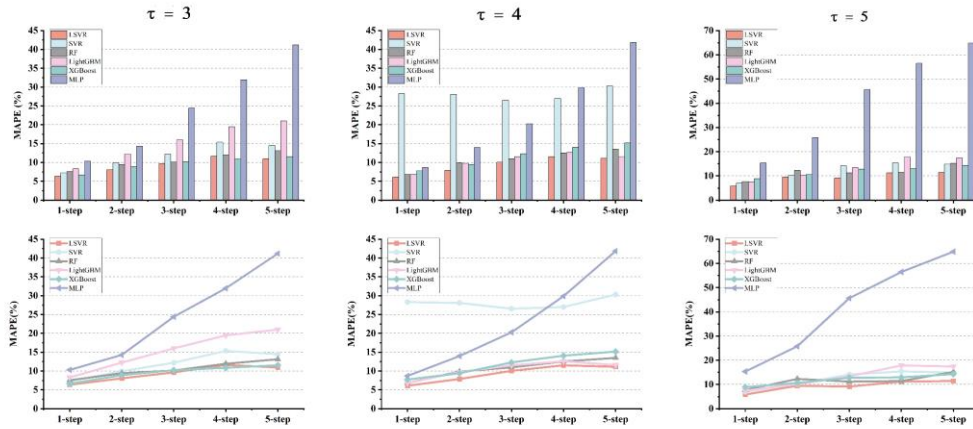
Table 1 *MAPE*(%) of the forecasting models

	Steps	<i>LSVR</i>	<i>SVR</i>	<i>RF</i>	<i>LightGBM</i>	<i>XGBoost</i>	<i>MLP</i>
$\tau = 3$	<i>step1</i>	5.844	6.966	7.728	7.444	8.913	15.372
	<i>step2</i>	9.504	10.193	12.301	10.167	10.637	25.778
	<i>step3</i>	9.138	14.148	11.190	13.419	12.804	45.638
	<i>step4</i>	11.199	15.376	11.424	17.868	12.938	56.474
	<i>step5</i>	11.418	14.914	15.193	17.450	14.291	64.856
$\tau = 4$	<i>step1</i>	6.368	7.264	7.548	8.286	6.628	10.296
	<i>step2</i>	8.069	9.955	9.414	12.249	8.892	14.273
	<i>step3</i>	9.632	12.218	10.142	16.000	10.217	24.397
	<i>step4</i>	11.622	15.345	11.927	19.467	10.870	31.967
	<i>step5</i>	10.932	14.487	13.120	21.004	11.538	41.182
$\tau = 5$	<i>step1</i>	6.114	28.309	6.823	6.799	7.746	7.746
	<i>step2</i>	7.874	28.077	9.863	9.729	9.403	9.403
	<i>step3</i>	10.058	26.557	10.972	11.534	12.287	12.287
	<i>step4</i>	11.532	27.004	12.557	12.585	14.067	14.067
	<i>step5</i>	11.118	30.294	13.497	11.588	15.163	15.163

256

257 **Figure 4** is when $\tau=5$, the output value of the machine learning model after data
 258 reconstruction, a total of 95 points, the comparison between the predicted value of the 6
 259 models and the original value. It can be seen that the effect of *SVR* is a bit worse, and there
 260 is a phenomenon of underfitting in the training set, lead to poor prediction results in the test
 261 set. *MLP* has a certain overfitting phenomenon, over-learning the information of the data set,

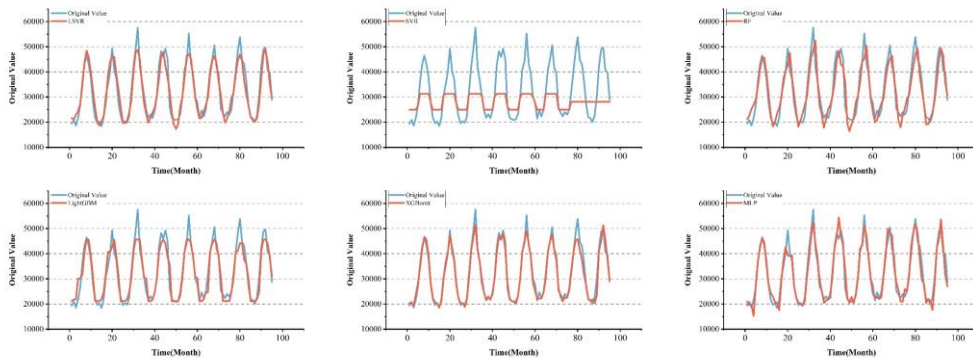
262 resulting in very complicated results in the training set. The best performance on the training
 263 set is *GWO-XGBoost*, but his prediction results are slightly worse than *GWO-LSVR*.
 264



265
 266 **Figure 3 MAPE results for a 5-step forecast with 3 time lags**
 267

265
 266
 267
 268
 269
 270
 271

To sum up, the proposed *GWO-LSVR* hybrid model can get very good forecasting results
 whether it is the training set or the test set, and the obtained *MAPE* is also the best among
 all comparison models, with strong generalization performance and robust.



272
 273 **Figure 4 Predict data when $\tau=5$**
 274

272
 273
 274
 275
 276
 277

4.2 Discussion

278 In this section, we discuss the impact of different swarm intelligence optimization algorithms
 279 on the performance of *LSVR* models. Similar to *GWO*, *WOA* is also widely used to solve the
 280 problems of complex nonlinear systems. The following are the specific discussion results.
 281

282 Under three time lags, the 5-step forecasting is performed respectively, and the detailed
 283 *MAPE* results generated by *GWO-LSVR* and *WOA-LSVR* are listed in **Table 2**. Under the
 284 combination of three time lags and five forecasting steps (15 cases in total), *WOA* produces
 285 only two results that are slightly better than *GWO*.
 286

287 Both *WOA* and *GWO* can produce relatively small *MAPE* results in the first and second steps,
 288 but from the third step onwards, the results produced by *WOA* are larger than those of *GWO*,
 289 and the gap gradually increases. The smallest difference is $\tau=4$ at the first step, which is only

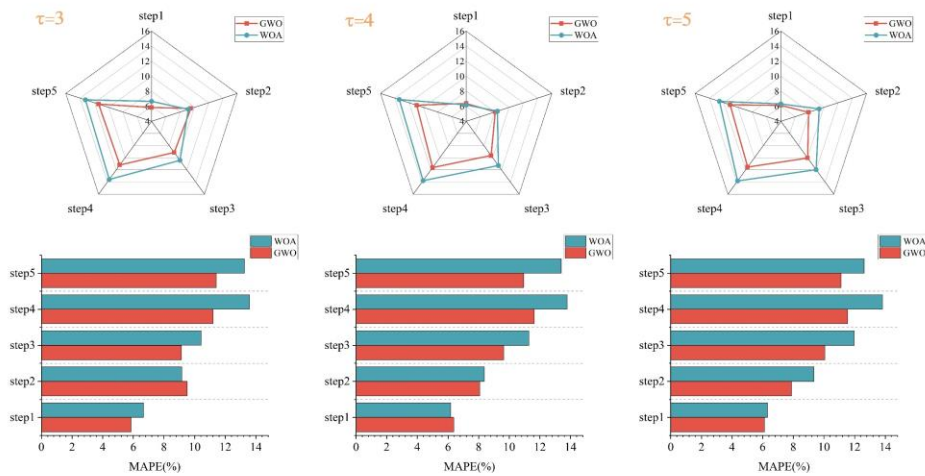
290 0.187%, and the largest difference is $\tau=4$ at the fifth step, with a difference of 2.451%. The
 291 detailed results presented in **Figure 5**.

292
 293
 294

Table 2 MAPE results of *GWO-LSVR* and *WOA-LSVR*

optimizer	Lag	step1	step2	step3	step4	step5
<i>GWO</i>	$\tau = 3$	5.844	9.504	9.138	11.199	11.418
	$\tau = 4$	6.368	8.069	9.631	11.622	10.932
	$\tau = 5$	6.114	7.874	10.058	11.532	11.118
<i>WOA</i>	$\tau = 3$	6.661	9.157	10.433	13.576	13.261
	$\tau = 4$	6.181	8.366	11.279	13.776	13.383
	$\tau = 5$	6.317	9.350	11.970	13.816	12.614

295



296
 297

Figure 5 MAPE results yield by *GWO-LSVR* and *WOA-LSVR*

298 **5. Conclusion**

299 Under the influence of the Russia-Ukraine war, there are energy tensions in Europe,
 300 especially the shortage of natural gas. Accurate forecasting of natural gas consumption is
 301 necessary.

302

303 This paper uses the Lagrangian Support Vector Regression model with the *Sorensen* kernel,
 304 combined with the Grey Wolf Optimizer and Nonlinear Auto-Regressive model, for multi-step
 305 forecasting of monthly natural gas consumption, based on the out-of-sample holdout
 306 validation. The proposed model was applied to forecast the total monthly natural gas
 307 consumption of 27 countries within Europe. Comparing the model with *SVR*, *RF*, *LightGBM*,
 308 *XGBoost*, and *MLP*'s five combined models based on *GWO*. It's find that the *GWO-LSVR* has
 309 the best generalization performance and most robust of all hybrid models. The *MAPE* yield
 310 by *GWO-LSVR* of each step at three time lags are from 5.844% to 11.622%. It also discussed
 311 the difference of the *GWO* and *WOA*, and find that *GWO* can better optimize the model
 312 hyperparameters in most cases. It can be concluded that the proposed *GWO-LSVR* model
 313 can be used to accurately predict natural gas consumption, and has strong generalization
 314 performance and robustness.

329 **REFERENCES**

- 330 [1] K. Tang, H. Li, and Z. Qian, "Forecasting Study of Natural Gas
Consumption by 331 Combined Models Based on LASSO and WOA", ARJOM, vol. 19, no.
1, pp. 23-31, Jan. 332 2023.
- 333 [2] Yang H-M, Pan C-S, Bai W. A review of time series forecasting methods[J].
Computer 334 Science, 2019, 46(1): 21-28.
- 335 [3] Box Q E P, Jenkins G M. Time series analysis: forecasting and control [M] .
San 336 Francisco: Holden-day Press,1970.
- 337 [4] Hannan E J. The estimation of the order of an ARMA process [J] . Ann.
Statist., 338 1980,8(5): 1071-1081.
- 339 [5] Boker J, Keviczky L. Structural properties and structure estimation of vector
difference 340 equations [J] . Int. J. Control, 1982, 36(3): 461-476.
- 341 [6] Deng Zili, Guo Xinxin. Dynamic system analysis and its applications [M].
Shenyang: 342 Liaoning Science and Technology Press, 1985, 31-130.
- 343 [7] Wang Xiaodong, Huang Kun. A neural network approach to natural gas
consumption 344 forecasting[J]. Natural Gas Exploration and Development, 2007, 30(3):
70-72.
- 345 [8] V Vapnik. The nature of statistical learning theory [M] . New York: Springer
Verlag 346 Press, 1995.
- 347 [9] Ping-Feng Pai, Wei-Chiang Hong. Support vector machines with simulated
annealing 348 algorithms in electricity load forecasting [J] . Energy Conversion and
Management, 349 2005, 46: 2669-2688.
- 350 [10] Ping-Feng Pai, Chih-Sheng Lin. A hybrid ARIMA and support vector machines
model in 351 stock price forecasting [J] . Omega, 2005, 33(6):497-505.
- 352 [11] J L Rojo-Álvarez, G Camps-Valls, M Martínez-Ramón, et al. Support vector machines
353 framework for linear signal processing [J] . Signal Processing, 2005, (85):2316-2326.
- 354 [12] Mei Hu, Liang Guizhao, Zhou Yuan, Li Zhiliang. A study of support vector machines for
355 quantitative constitutive relationship modeling [J]. Science Bulletin, 2005, 50(16):1703-
356 1708.
- 357 [13] Cheng Jun-Sheng, Yu De-Suke, Yang Y. A support vector regression machine based
358 approach to the Hilbert Huang transformation endpoint effect problem [J]. Journal of
359 Mechanical Engineering, 2006, 42(4): 23-31.
- 360 [14] Wang, T. H., Chen, J. T.. A review of research on the selection of kernel functions[J].
361 Computer Engineering and Design, 2012, 33(3): 1181-1186.
- 362 [15] Feng, K.-H. Comparison of SVM classification kernel functions and parameter
363 selection[J]. Computer Engineering and Applications, 2011, 47(3): 123-124.

